DOI: 10.15826/chimtech.2015.2.4.030

N. V. Kosova, O. A. Podgornova
Institute of Solid State Chemistry and Mechanochemistry SB RAS,
Kutateladze 18, 630128 Novosibirsk, Russia
*Tel: +7 383 2332410*1115*
Fax: +7 383 3322847
E-mail: kosova@solid.nsc.ru

Supervalent doping of $LiFePO_4$ for enhanced electrochemical performance*

Vanadium and titanium doped orthophosphates $LiFe_{0.9}M_{0.1}PO_4$ with an olivine-type structure (space group Pnma) were prepared by mechanochemically assisted solid state synthesis using a high-energy AGO-2 planetary mill and post-annealing at 750 °C. It has been established that the V and Ti ions do not fully substitute for Fe^{2+} in the $LiFePO_4$ structure. The other part of these ions participate in the formation of the secondary phases with the open Nasicon-type structures: monoclinic $Li_3V_2(PO_4)_3$ (space group $P2_1/n$) and rhombohedral $LiTi_2(PO_4)_3$ (space group $R\text{-}3c$). According to TEM, the average particle size of the nanocomposites is about 100–300 nm. EDX microanalysis reveals that the small particles of the secondary phases are segregated on the surface of the larger $LiFePO_4$ particles. On the charge-discharge profiles of LiFe0.9M0.1P04, the plateaus corresponding to $LiFePO_4$ and the secondary phases are observed. V doping improves cycleability and rate capability of $LiFePO_4$ to a greater extent than Ti.

Keywords: $LiFePO_4$; supervalent doping; mechanical activation; electrochemical cycling

*This work is executed at partial financial support of RFBR (grant № 14-03-01082).

Introduction

Many efforts have been made to turn insulating compounds into attractive electrode materials, including nanosizing, carbon nanopainting and metal doping [1–3]. This allows the olivine-type lithium iron phosphate $LiFePO_4$ with inherent low electronic conductivity and slow lithium diffusion [3, 4] to become a promising cathode material exhibiting favorable electrochemical properties and to be commercialized. Li ions migration in $LiFePO_4$ is found to occur preferably down the [010] channels, following a curved trajectory. The most favorable intrinsic defects in $LiFePO_4$ are the cation antisite defects, in which Li and Fe ions exchange positions. According to *ab initio* simulations of the $LiFePO_4$ doping, low favorable energies are found only for divalent dopants on the Fe sites, whereas substitution energy for supervalent cations is energetically unfavorable [5]. Meanwhile, it has been

shown experimentally that supervalent doping of $LiFePO_4$ on Li sites increases its electronic conductivity by a factor of ~108 and results in superior electrochemical performance [3]. Later on, these results were explained by the formation of the conductive impurity phases. The studies on the enhancement of life stability and rate capability of $LiFePO_4$ are still highlighted.

Vanadium and titanium are very attractive dopants for $LiFePO_4$ since they readily form corresponding lithium metal phosphates. Although several reports have been published on vanadium [6-12] and titanium [13-16] substitution, there is much disagreement regarding the formation of the $LiFe_{1-y}V_yPO_4$ and $LiFe_{1-y}Ti_yPO_4$ solid solutions. Some authors insist that V^{3+} substitutes for Fe^{2+} on Fe sites within the solid solubility limit $0<x<0.08$ [9] or at $x<0.1$ [7]. According to [7], the solid-solution limit depends on the preparation method and heat-treatment temperature. When synthesis temperature is increased to 700 °C, the decreased V solubility and the formation of the second phase – $Li_3V_2(PO_4)_3$ – are observed. Similarly, when LiFePO4 was doped with Ti, titanium phosphate impurities like TiP_2O_7 and $LiTi_2(PO_4)_3$ at higher doping level ($y>0.05$) were formed [14]. V- and Ti-doped $LiFePO_4$ samples are reported to show excellent reversible capacity and rate capability. However, there is no common viewpoint on the mechanism of the improvement. In many previous studies, cationic substitution to the Fe site (M2 site) in $LiFePO_4$ usually results in higher ionic mobility and Li_+ diffusion coefficient due to the cell volume expansion and the probable weakening of the Li-O interactions. The latter lowers the charge transfer resistance and thus improves the reversibility of the lithiation process. Only a limited number of reports show that cationic substitution to the Li site (M1 site) is probable, resulting in the production of Li vacancies that increases the capacity of LiFePO4 [11]. It remains essential to develop the synthetic routs with an appropriate cation doping of $LiFePO_4$ along with decreased particle size and optimized carbon coating.

The aim of the present work was the study of V- and Ti-doping of $LiFePO_4$ prepared by mechanochemically assisted carbothermal reduction.

Experimental

Li_2CO_3, Fe_2O_3, V_2O_5, TiO_2 and $(NH_4)_2HPO_4$ were used as reagents for the synthesis of $LiFe_{0.9}V_{0.1}PO_4$ and $LiFe_{0.9}Ti_{0.1}PO_4$, further labeled as LFVP and LFTP. Soot was used as a reducing and coating agent (5%). The reagent mixtures were undergone a mechanochemical activation (MA) by means of a high-energy AGO-2 planetary mill (900 rpm). The activated mixtures were annealed at 750 °C in Ar flow.

X-Ray powder diffraction (XRD) was performed using D8 Advance Bruker diffractometer, Cu*K*α irradiation. The structural refinement of the XRD data was carried out by the Rietveld method using the GSAS software package. Particle size and morphology were characterized by transmission electron microscopy (TEM) using a JEM-2200 FS transmission electron microscope. Microanalysis was performed by means of energy dispersive X-ray analyzer EX-230 BU. For electrochemical testing,

the composite cathodes were fabricated using 75 wt.% active material, 20 wt.% Super P (conductive carbon) and 5 wt.% PVDF/NMP binder. The as-mixed slurry was then pasted on the aluminum foil to obtain working electrodes. The loading density of the prepared samples was 2–3 mg·cm^{-2}, and the electrode diameter of 10 mm was used throughout. The working electrodes were dried at 120 °C. Swagelok-type cells were assembled in an argon-filled glove box with Li as an anode, 1M $LiPF_6$ solution in a mixture of ethylene carbonate and dimethylcarbonate (1:1 by weight) as an electrolyte, and a glass fiber filter (Whatman, Grade GF/C) as a separator.

Results and discussion

Figure 1 shows the Rietveld refined XRD patterns of the as-prepared samples LFVP and LFTP. It is evident that both of them are well fitted by a two-phase model: LFP with an orthorhombic olivine-type structure (space group *Pnmb*) and LVP with a monoclinic structure (space group $P2_1/n$) or LTP with a rhombohedral structure (space group *R-3c*). The observed and calculated patterns match well, and the reliability factor (R_w) is good. The olivine structure of LFP consists of corner-shared FeO6 octahedra running parallel to the *b*-axis, which are linked together by the PO_4 tetrahedra. The monoclinic structure of LVP comprised of metal octahedra and phosphate tetrahedra sharing oxygen vertices. Li ions are situated in the cavities within the framework [17]. The occurrence of corner-shared chains of Li polyhedra along the b-axis and open diffusion pathways in the other directions provide rapid, isotropic ionic transport similar to the fast-ion conduction in NASICON phases. The rhombohedral structure of LTP consists of a three-dimensional network made of TiO_6 octahedra sharing all their corners with PO_4 tetrahedra and *vice versa* to form so-called 'lantern units', all oriented in the same direction (along the c-axis) [18]. The conduction channels are generated along the c-axis direction. The results of structural analysis of the composites obtained from XRD Rietveld refinement are shown in Table 1. The lattice parameters of LFP in the LFVP composite are slightly smaller than those of pure LFP. The slight changes of lattice parameters can be ascribed to the small incorporation of V ions with smaller ionic radius (R_{V3+}=0.64 Å, R_{V4+}=0.53 Å) into the structure of LFP. The calculated mol.% of LFP and LVP phases are about 96.3 and 3.7 mol.%, respectively. In the LFTP composite, the changes of lattice parameters

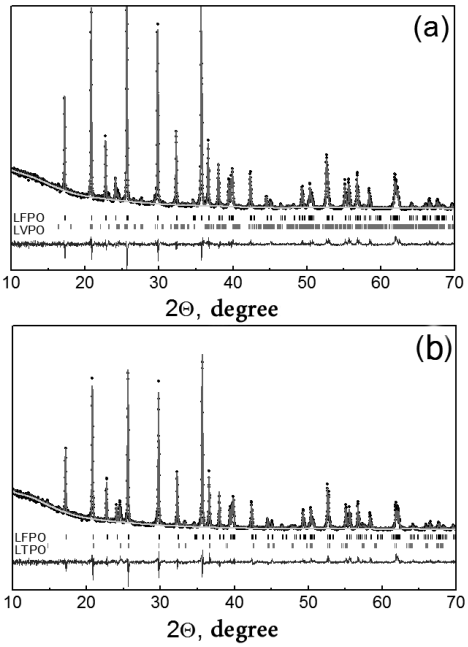

Fig. 1. Rietveld refined XRD patterns o f V- (a) and Ti-doped (b) $LiFePO_4$

Table 1

Results of structural analysis obtained from XRD Rietveld refinement

Lattice parameters	LFP	LFVP		LFTP	
		LFP	LVP	LFP	LTP
a, Å	10.3052(1)	10.2935(3)	8.583(6)	10.3053(3)	8.491(2)
b, Å	5.9946(1)	5.9886(1)	8.574(6)	5.9947(2)	8.491(2)
c, Å	4.6833(1)	4.6843(1)	12.018(8)	4.6828(1)	20.855(9)
□			90.56(6)		
V, Å^3	289.32(1)	288.76	884.4(7)	289.29(2)	1302.1(4)
R_{wp}, %	6.60	8.52		9.29	
χ^2	1.290	2.205		2.214	
LFP/LMP (mol. %)		96.3/3.7		95.8/4.2	

of LFP are smaller than in LFVP. The calculated LFP/LTP ratio is 95.8/4.2 mol.%, evidencing lower degree of Ti^{4+}/Fe^{2+} substitution.

Incorporation mechanism of supervalent ions in the structure of LFP is debatable. According to [5], it is unfavorable in all the $LiMPO_4$ systems. This strongly suggests that these ions are unstable within the crystal lattice of $LiMPO_4$ and unlikely to be incorporated beyond low concentration (>3%). The compensation mechanism for supervalent dopants was found to be the formation of M^{2+} vacancies, whereas compensation by a change in charge state of the transition metal ion was much higher in energy.

According to the literature, the electronic state of Fe ions in LFP does not change upon V- and Ti-doping. The authors of Refs. [13–15] have found the oxidation state of doped Ti ions as 4+, whereas the oxidation state of V ions is between 3+ and 4+ [9-11]. The M^{3+} and M^{4+} substitution for Fe^{2+} in the structure of LFP compound along with the formation of Li vacancies and 'anti-site' pair defects can be represented by the following equations in Kroger-Vink notation:

$$Li_{Li}^{x} \rightarrow V_{Li}^{'} + Li_i^{\bullet}$$

$$Fe_{Fe}^{x} + Li_{Li}^{x} \rightarrow LiFe' + Fe_{Li}^{\bullet}$$

$$1/2M_2O_3 + 3/2Fe_{Fe}^{x} \rightarrow M_{Fe}^{\bullet} + 1/2V_{Fe}^{''} + 3/2FeO$$

$$MO_2 + 2Fe_{Fe}^{x} \rightarrow M_{Fe}^{\bullet\bullet} + V_{Fe}^{''} + 2FeO$$

It was supposed that iron ions can migrate from $Fe_{Li}^{\bullet}$ sites to $V_{Fe}^{''}$ vacancies. Thus, the main defects in the V- and Ti-doped LFP should be Li vacancies and M^{n+} ions in Fe sites [5].

According to TEM, the LFVP and LFTP samples consist of the irregular shaped nanosized particles with an average particle size of about 100–300 nm similar to pure LFP (Fig. 2). The surface of the particles is coated by a thin carbon layer. EDX microanalysis confirms the targeted concentration of the elements in the as-prepared composites. The maps of Fe and V distribution in LFVP are shown individually and overlaid with the original image in Fig. 2c-e. It is evident that LVP forms smaller particles, preferably on the surface of larger LFP particles, thus, probably enhancing surface Li ion mobility in the composite.

Electrochemical behavior of LFVP and LFTP was studied within the 2.5–4.3 V voltage window at C/10 charge-discharge rate. Charge-discharge profiles and the correspondent d*Q*/d*V* vs. voltage plots

are shown in Fig. 3. The profiles, as well as the number and the position of the redox peaks agree with the literature data for the pure phases. The plateau at around 3.4 V is based on the Fe^{2+}/Fe^{3+} redox couple corresponding to one Li (de)intercalation from/in LFP *via* a two-phase mechanism. V-doped sample is characterized by the appearance of some additional distinct plateaus at higher voltage, which have been attributed to the operation of V3+/V^{4+} and V^{4+}/V^{5+} couples in LVP. According to Ref. [17], LVP exhibits three oxidation plateaus around 3.62, 3.70, and 4.09 V when charged to 4.3 V, corresponding to a sequence of two-phase transitions $Li_3V_2(PO_4)_3 \rightarrow Li_{2.5}V_2(PO_4)_3 \rightarrow Li_2V_2(PO_4)_3 \rightarrow Li_1V_2(PO_4)_3$. Very close position of the oxidation and reduction peaks for pure LVP upon cycling in the 2.5–4.3 V points to low degree of polarization and that the electron and ion transport is facile [17]. Ti-doped LFP also exhibits additional plateau, but at lower voltage. This plateau was ascribed to operation of the Ti4+/Ti3+ couple in LTP. It has been found earlier that LTP can insert two additional Li ions at ~2.5 V corresponding to reduction of two Ti^{4+} ions to Ti^{3+} [19]. Li insertion in LTP is realized by a two-phase mechanism. It should be emphasized that LTP serves as an insertion host to accommodate the Li ions that could not be inserted back into the LFP structure. Note that the position of the redox peaks on the d*Q*/d*V* plots well corresponds to those of pure LFP, LVP and LTP, evidencing that low degree of substitution and the composite formation do not noticeably influence voltage of the redox processes upon cycling. On the contrary, in the case of the olivine-type solid solutions, e.g., $LiFe_{1-y}Mn_yPO_4$ and $LiFe_{1-y}Co_yPO_4$, the Fe2+/Fe^{3+}

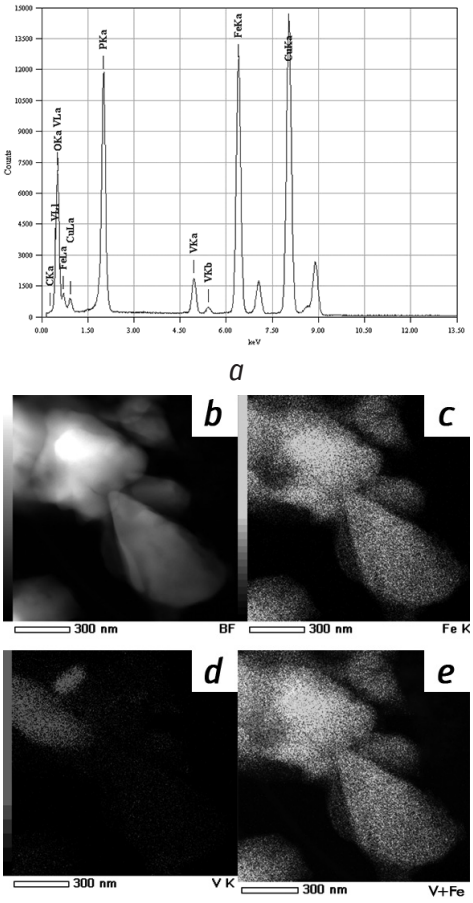

Fig. 2. EDX (a), TEM (b) and element distribution images (c-e) of V-doped $LiFePO_4$.

and Mn^{2+}/Mn^{3+} (Co^{2+}/Co^{3+}) redox potentials progressively increase/decrease *vs.* dopant content [20, 21].

Figures 4a and 4b present discharge profiles of the doped samples at different rates, whereas Fig. 4c and 4d display the dependence of the specific discharge capacity *vs.* cycle number at C/10 rate and cycling rate, respectively. The initial discharge capacity was 152 $mAh \cdot g^{-1}$ for LFVP and 135 $mAh \cdot g^{-1}$ for LFTP, however it gradually decreases at the following cycles. Rate capability of LFVP is superior to that of LFTP. The enhancement of the

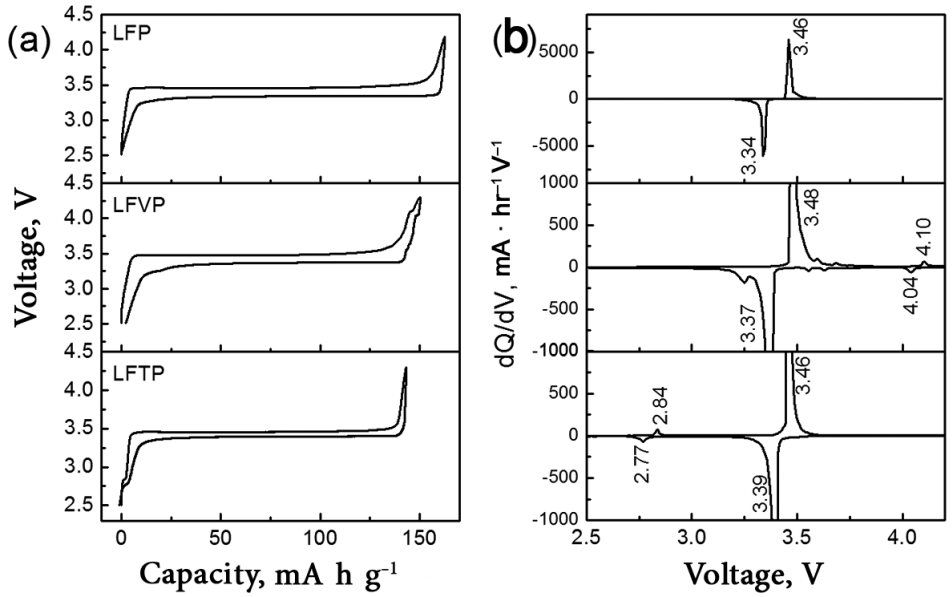

Fig. 3. Charge-discharge profiles (a) and dQ/dV vs. voltage plots (b) for pure, V- and Ti-doped $LiFePO_4$

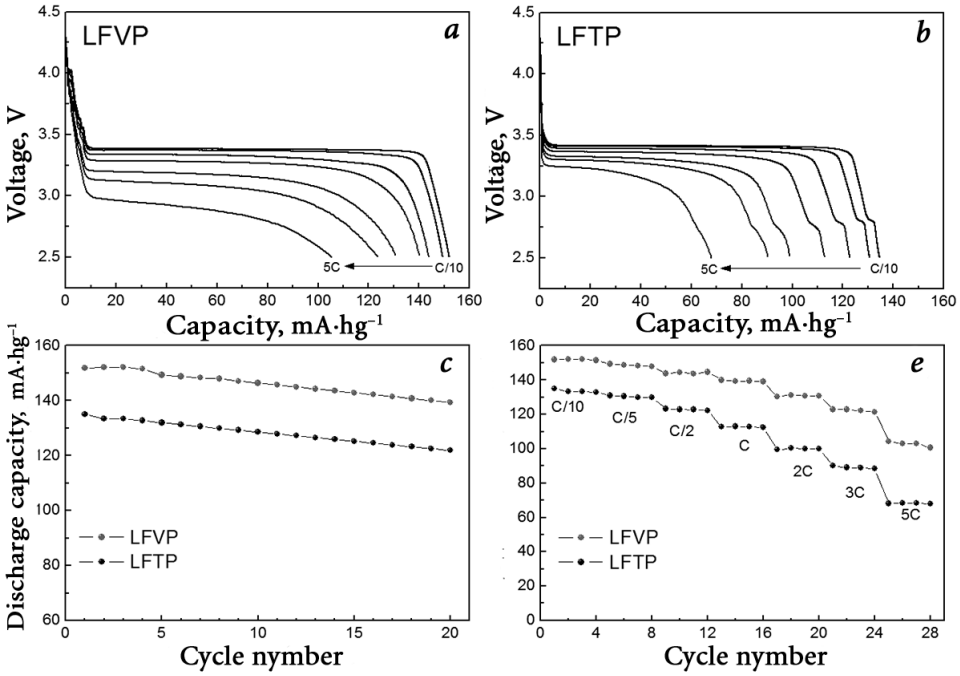

Fig. 4. Discharge profiles (a,b), specific discharge capacity vs. cycle number (c) and cycling rate (d) for V- and Ti-doped $LiFePO_4$

electrochemical performance of LFVP was considered to be a result of the presence of LVP phase with high Li ion mobility and suitable amount of point defects in the structure of LFVP.

Conclusion

V- and Ti-doped $LiFePO_4$ samples were synthesized using Fe_2O_3 and V_2O_5 or TiO_2 as the raw materials with carbon both as a reductive and covering agent by a simple mechanochemically assisted carbothermal reduction. It has been established that the as-prepared samples are comprised of two finely mixed phases: $LiFePO_4$ with a small degree of Fe/V(Ti) substitution and the impurity phases: $Li_3V_2(PO_4)_3$ or $LiTi_2(PO_4)_3$. Small particles of the secondary phases are segregated on the surface of larger $LiFePO_4$ particles. V-doped $LiFePO_4$ exhibits better cycleability and rate capability than Ti-doped one. This should be due to higher lithium diffusion arose from the presence of $Li_3V_2(PO_4)_3$ with high Li ion mobility and suitable amount of defects due to partial V substitution for Fe. The increase in a number of voltage plateaus and the mean intercalation voltage due to the presence of the $Li_3V_2(PO_4)_3$ secondary phase should be advantageous for improving the cell performance of $LiFePO_4$.

1. Yamada A., Chung S. C., Hinokuma K. Optimized $LiFePO_4$ for lithium battery cathodes. *J. Electrochem. Soc.* 2001;148(3):A224-A229.
2. Ravet N., Chouinard Y., Magnan J. F., Besner S., Gauthier M., Armand M. Electroactivity of natural and synthetic triphylite. *J. Power Sources.* 2001;97-98:503-507. doi: 10.1016/S0378-7753(01)00727-3.
3. Chung S. Y., Chiang Y. M. Microscale Measurements of the Electrical Conductivity of Doped $LiFePO_4$. *Electrochem. Solid-State Lett.* 2003;6(12):A278-A281.doi: 10.1149/1.1621289.
4. Prosini P. P., Lisi M., Zane D., Pasquali M. Determination of the chemical diffusion coefficient of lithium in LiFePO4. *Solid State Ionics.* 2002;148(1-2):45-51. doi: 10.1016/S0167-2738(02)00134-0.
5. Fisher C. A. J., Prieto V. M. H., Islam M. S. Lithium battery materials $LiMPO_4$ (M = Mn, transport Fe, Co, and Ni): Insights into defect association, mechanisms, and doping behavior.*Chem. Mater.* 2008;20(18):5907-5915. doi: 10.1021/cm801262x.
6. Wang L., Li Z., Xu H., Zhang K. *J. Phys. Chem. C.* 2008;112:308.
7. Omenya F., Chernova N. A., Upreti S., Zavalij P. Y., Nam K. W., Yang X. Q., Whittigham M. S. Can vanadium be substituted into $LiFePO_4$? *Chem. Mater.* 2011;23(21):4733-4740. doi: 10.1021/cm2017032.
8. Xiang J. Y., Tu J. P., Zhang L., Wang X. L., Zhou Y., Qiao Y. Q., Lu Y. Improved electrochemical performances of $9LiFePO_4{\cdot}Li_3V_2(PO_4)$/C composite prepared by a simple solid-state method. *J. Power Sources.* 2010;195(24):8331-8335. doi: 10.1016/j.jpowsour.2010.06.070.
9. Ma J., Li B., Du H., Xu C., Kang F. *J. Electrochem. Soc.* 2011;158:A26.
10. Zhang L. L., Liang G., Ignatov A., Croft M. C., Xiong X. Q., Hung I. M.,

Huang Y. H., Hu X. L., Zhang W. X., Peng Y. L. Effect of vanadium incorporation on electrochemical performance of LiFePO4 for lithium-ion batteries. *J. Phys. Chem. C.* 2011;115(27):13520-13527. doi: 10.1021/jp2034906.

11. Chiang C. Y., Su H. C., Liu P. J., Hu C. W., Sharma N., Peterson V. K., Hsieh H. W., Lin Y. F., Chou W. C., Lee C. H., Lee J. F., Shew B. Y. Vanadium substitution of $LiFePO_4$ cathode materials to enhance the capacity of LiFePO4-based lithium-ion batteries. *J. Phys. Chem. C.* 2012;116(46):24424-24429. doi: 10.1021/jp307047w.
12. Zhong S., Wu L., Liu J. *Electrochim. Acta.* 2012;74:8.
13. Wang G. X., Bewlay S., Needham S. A., Liu H. K., Liu R. S., Drozd V. A., Lee J. F., Chen J. M. Synthesis and characterization of $LiFePO_4$ and $LiTi_{0.01}Fe_{0.99}PO_4$ cathode materials. *J. Electrochem. Soc.* 2006;153(1):A25-A31. doi: 10.1149/1.2128766.
14. Wang Z. H., Pang Q. Q., Deng K. J., Yuan L. X., Huang F., Peng Y. L., Huang Y. H. *Electrochim. Acta.* 2012;78:576.
15. Fang H., Liang G., Zhao L., Wallace T., Arava H., Zhang L. L., Ignatov A., Croft M. C. *J. Electrochem. Soc.* 2013;160:A3148.
16. Koenig G. M., Jr., Ma J., Key B., Fink J., Low K. B., Shahbazian-Yassar R., Belharouak I. Composite of $LiFePO_4$ with titanium phosphate phases as lithium-ion battery electrode material. *J. Phys. Chem C.* 2013;117:21132. doi:10.1021/p4074174.
17. Huang H., Yin S. C., Kerr T., Taylor N., Nazar L. F. Nanostructured composites: A high capacity, fast rate $Li_3V2(PO_4)3$/carbon cathode for rechargeable lithium batteries. *Adv. Mater.* 2002;14(21):1525–1528. doi: 10.1002/1521-4095 (20021104) 14;21<1525:AID-ADMA1525>3.0.co;2–3.
18. Belous A. G., Novitzkaya G. N., Polyanetzkaya S. V., Gornikov Yu. I. Study of Complex Oxides of Composition La//2////3// minus //xLi//3//xTiO//3. *Russ. Izvestiya AN SSSR, Neorgan. Materialy.* 1987;23(3):470–472.
19. Patoux S., Masquelier C. Lithium insertion into titanium phosphates, silicates, and sulfates. *Chem. Mater.* 2002;14(12):5057-5068. doi: 10.1021/cm0201798.
20. Kosova N. V., Devyatkina E. T., Slobodyuk A. B., Petrov S. A. Submicron $LiFe_{1-y}Mn_yPO_4$ solid solutions prepared by mechanochemically assisted carbothermal reduction: The structure and properties. *Electrochim. Acta.* 2012;59(1):404-411. doi : 10.1016/j.electacta.2011.10.082.
21. Kosova N. V., Podgornova O. A., Devyatkina E. T., Podugolnikov V. R., Petrov S. A. Effect of Fe^{2+} substitution on the structure and electrochemistry of $LiCoPO_4$ prepared by mechanochemically assisted carbothermal reduction. *J. Mater. Chem. A.* 2014;2(48):20697-20705. doi: 10.1039/c4ta04221b.